processes

MDPI

Article

Quality and Microstructural Changes in Salted Goose Meat Dried by Hot-Air, Infrared, and Microwave Techniques

Emre Kabil [1,*], Muhammet Ali Çakır [2], Barış Yalınkılıç [3] and Mehmet Başlar [4]

[1] Department of Food Processing, Armutlu Vocational College, Yalova University, 77500 Yalova, Türkiye
[2] Department of Nutrition and Dietetics, Faculty of Health Science, Kırklareli University, 39000 Kırklareli, Türkiye; m.ali.cakir@klu.edu.tr
[3] Department of Gastronomy and Culinary Arts, Faculty of Architecture and Design, İstanbul Gedik University, 34876 Istanbul, Türkiye; baris.yalinkilic@gedik.edu.tr
[4] iPeak Academy Ltd., Mildenhall, Suffolk IP28 7DE, UK; mehmetbaslar@ipeakacademy.com
* Correspondence: emre.kabil@yalova.edu.tr

Abstract

This study aimed to investigate the effects of different drying methods on salted goose meat, with a particular focus on its microstructure, drying kinetics, color, TBARS (Thiobarbituric acid reactive substances), rehydration, and shrinkage parameters. Goose breast meat with 6% (*w*/*w*) salt was dried using hot air and infrared drying at temperatures of 55 °C, 65 °C, and 75 °C, as well as microwave at power levels of 120 W, 350 W, and 460 W. The results revealed that increasing temperature and power levels increased the drying rate in all drying methods. The microwave-dried samples at 460 W and 350 W showed the highest average *L** values, followed by the samples dried at 75 °C using infrared and hot air. On the other hand, the lowest temperature (55 °C) and power (120 W) levels resulted in the highest average TBARS values across all drying processes. Furthermore, the highest shrinkage rate was observed at the highest temperature (75 °C) or power level (460 W), while the highest average rehydration rate was recorded in the samples dried at 75 °C using infrared and hot air. Considering the microstructure of the dried meats, the drying method and the temperature/power conditions were found to cause a change in the fibril structures to varying extents.

Keywords: goose meat; drying kinetics; microwave drying; infrared drying; meat microstructure

check for updates

Academic Editors: Nikola Čobanović and Nevena Grković

Received: 19 August 2025
Revised: 4 October 2025
Accepted: 5 October 2025
Published: 10 October 2025

Citation: Kabil, E.; Çakır, M.A.; Yalınkılıç, B.; Başlar, M. Quality and Microstructural Changes in Salted Goose Meat Dried by Hot-Air, Infrared, and Microwave Techniques. *Processes* **2025**, *13*, 3223. https://doi.org/10.3390/pr13103223

Copyright: © 2025 by the authors. Licensee MDPI, Basel, Switzerland. This article is an open access article distributed under the terms and conditions of the Creative Commons Attribution (CC BY) license (https://creativecommons.org/licenses/by/4.0/).

1. Introduction

Drying is a fundamental food preservation technique based on reducing the water activity, an indicator of food perishability caused by microorganisms. This control over microbiological, biochemical, and chemical activities is achieved through the removal of water from the product under hygienic conditions [1,2]. Historically, food preservation through drying relied on natural techniques. However, with the advent of industrialization, hot air drying—a method that has many advantages over natural approaches—has emerged as a widespread technique of food preservation. Recent studies focused on developing alternative methods to replace traditional natural drying and conventional hot air drying [3,4] and highlight infrared and microwave drying methods [5–7].

In recent years, in the search for improving drying efficiency and product quality, different drying methods have been increasingly investigated as alternatives to conventional techniques. Infrared drying is notable for its rapid performance, facilitated by the direct

absorption of infrared rays, eliminating the need to heat the drying chamber [8]. This technique offers several advantages, including reduced energy consumption, cost-effectiveness, and improved product quality, all of which position it as a promising emerging drying methodology [6,9]. Microwave technology, a modern approach used in various stages of food production, operates on the principle of heat release through molecular mobility via electromagnetic waves within the frequency range of 300 MHz to 300 GHz [10]. Microwave drying offers distinct advantages over traditional hot air drying, including significantly reduced heating times and decreased energy consumption, especially for products with lower water content [11,12]. Drying meat, a highly perishable food, is important both for processing it into new products and for extending its shelf life. In addition, meat drying is frequently used in combination with processes such as salting, curing, or smoking [13–15]. Dried beef, fish, and poultry are among the important meat products preferred in some countries [16].

Goose meat represents an economically important product within the poultry sector. According to FAOSTAT, China is the world's largest producer of goose meat and accounts for 89% of global goose stock and 95% of goose production [17]. Furthermore, Hungary and Poland continue to play a significant role as major producers of goose meat [18]. Other major goose meat producers include Myanmar, the Russian Federation, Ukraine, Madagascar, Egypt, and Türkiye [19]. In Türkiye, goose meat production is mostly concentrated in the high-altitude Northeastern Anatolia region, characterized by long, cold, and harsh winters [20].

Goose (*Anser anser*) is a widely consumed poultry species in different cultures. Goose meat has been processed in various cuisines across different countries, giving rise to the widely recognized products like Weihnachtsgans from Germany, roast goose from Hong Kong, and "Martinjska guska s marunima" from Croatia [21]. An example of goose meat in Türkiye is salted and dried goose meat, which is traditionally produced in the provinces of Kars (altitude: 1756 m) and Ardahan (altitude: 1900 m) in the fall, especially just following the snowfall. For inhabitants of this geographical region, where the snow cover persists for several months, salted and dried goose meat serves as a crucial source of protein and an important food supply during the extended winter period.

Goose meat is known for its high levels of unsaturated fatty acids, particularly oleic acid, making it a potentially valuable source of fat-soluble nutrients. In addition, it serves as an important supplier of essential amino acids in the human diet [22]. By implementing traditional meat processing techniques (e.g., curing, drying, salting, etc.) commonly used for beef, goose meat can also be transformed into products like polgesek [23], fermented sausage [24], and salami [25], all of which offer enhanced sensory characteristics and improved shelf life.

As in other meats, goose meat is also susceptible to microbial spoilage, a characteristic that compromises the effectiveness of the natural drying method that, in addition to taking a long time, has a temperature range suitable for microbial growth. By contrast, technological methods offer a more reliable option to prevent spoilage. Salting processes causing osmotic water loss through salt diffusion into the tissue are known to affect several physicochemical parameters of meat [26,27]. Taking into account the advantages of salting processes, it is important to examine the effectiveness of various drying techniques for salted goose meat compared to traditional methods, particularly in terms of both drying kinetics and physicochemical changes in the product. Previous studies on poultry meat documented that the amount of connective tissue proteins in goose and turkey is lower as compared to broiler and duck meat, while the total lipid content in goose breast meat exceeds that of broiler, turkey, and duck breast meat [28]. During the drying of poultry meat, moisture must diffuse through the connective tissue layers located in the endomysial, perimysial,

and epimysial regions before being released from the product [29]. The shrinkage behavior of connective tissue during drying affects the pore structure of the meat, thereby directly impacting moisture migration [30]. The efficiency of the drying process is also affected by variations in intramuscular fat content [3]. Considering the potential effect of differences in muscle chemical composition on drying behavior, it is evident that drying kinetics should be investigated separately for each poultry species. However, although drying techniques have been widely and successfully applied to poultry meats such as chicken and turkey to accelerate moisture removal and maintain quality [31,32], to the best of our knowledge, none of the previous studies has addressed the application of hot-air, infrared, and microwave drying techniques to salted goose meat.

To fill this gap in the literature, the present study aimed to comparatively investigate the effects of Hot Air Drying (HAD), Microwave Drying (MD), and Infrared Drying (ID) techniques on the physicochemical quality parameters and drying kinetics of goose meat. To this end, TBARS values, color parameters, microstructure, shrinkage, and rehydration rates of the samples were analyzed, and the drying kinetics were evaluated using nine different mathematical models.

2. Materials and Methods

2.1. Raw Material and Salting Process

The present study was conducted using female geese (n = 36) obtained from a goose farm in Göle district, Ardahan, Türkiye. After slaughtering the birds, their breast meat, separated from carcasses, was purchased and transported to the laboratory in a cooler. The breast meat was then separated from the skin. After skinning, samples were taken from the raw meat for analysis, and the remaining breast meat was subjected to dry-salting with rock salt at 6% (w/w; 6 g NaCl per 100 g meat) by rubbing uniformly onto all surfaces. After salting, the meat was vacuum-packaged and equilibrated at 4 °C for 24 h before drying.

2.2. Drying Process with Different Techniques

Salted meats were cut into 3 × 3 × 1 cm pieces and dried to a constant moisture content using three different methods—HAD, MD, and ID. The drying endpoint was determined by the moisture rate (MR), and a value of 0.1 was used as the approximate MR. The average MR after drying was determined to be 0.117 ± 0.019. For HAD, the salted meats were dried in an oven (WiseVen Wof-155, Daihan Scientific Co., Seoul, Republic of Korea) at 55, 65, and 75 °C under constant air flow. In the case of ID, the drying was carried out in a halogen lamp infrared dryer (And Mx-50, A&D Company, Tokyo, Japan) at 55, 65 and 75 °C. Finally, for MD, the drying process was carried out using a microwave oven (Md 574 S, Arçelik A.Ş., İstanbul, Türkiye) at 120, 350, and 460 W power. Drying kinetics were characterized at different temperatures and microwave power levels; in addition, drying was continued until the moisture content reached 25% on a wet basis.

2.3. Sampling

For the characterization of the proximate composition, TBARS, color, and pH of the raw goose meat, samples were taken from each muscle before processing. Following the salting process, samples were taken from the salted breast meat for TBARS analysis. During the drying of the salted meat, the necessary data for drying kinetics were collected. After drying, dehydrated samples were used for determination of TBARS, color, and calculation of shrinkage and rehydration rates.

2.4. Dry Matter, Ash, Fat Content, and pH

The dry matter, ash, protein, and fat contents were analyzed using the procedures of AOAC previously described by Gökalp et al. [33]. Dry matter was determined by oven drying until constant weight at 105 ± 2 °C. The ash was determined by holding it to a constant weight at 550 ± 10 °C after pre-drying. Total fat content was determined by Soxhlet extraction using petroleum ether for 6–8 h. Protein content was analyzed with the Kjeldahl method using a factor of 6.25 for nitrogen. For pH measurement, 5 g of minced raw material were weighed, and 50 mL of distilled water was added to each sample. The mixtures were then homogenized using an Ultra-Turrax (Wisetis Hg-15d, Daihan Co., Seoul, Republic of Korea) for 1 min. Subsequently, the pH values of the homogenized samples were measured using a calibrated pH meter (HI 2211, Hanna Instruments, Woonsocket, RI, USA).

2.5. Thiobarbituric Acid Reactive Substance (TBARS) Analysis

To determine malondialdehyde (MDA) content, 2 g of the dried samples were mixed with a 12 mL TCA solution (7.5% TCA, 0.1% EDTA, 0.1% Propyl gallate dissolved in 3 mL ethanol) and homogenized using an Ultra-Turrax (Daihan Wisetis Hg-15d) for 15–20 s. After filtration (Whatman 1), 3 mL of the filtrate were collected, and 3 mL of TBA solution (0.02 M) was added. The mixture was then heated in a boiling water bath (100 °C) for 40 min. Afterwards, the mixture was cooled in cold water for 5 min and subsequently centrifuged (TDZ5-WS, Xiangyi Centrifuge Instrument Co., Hunan, China) at 2000× g for 5 min. The supernatant's absorbance at 530 nm was measured using a spectrophotometer (Jenway 6300, Staffordshire, UK), following Lemon's [34] method. TBARS were expressed as mg MDA/kg product at the end of drying. In addition, TBARS analysis was also conducted on raw meat and salted meat.

2.6. Color Parameters

The cross-sectional surface color intensities of the raw, salted, and dried meats were measured using a colorimeter (Wr-10, FRU, Shenzhen, China) with an 8 mm diameter aperture, D65 illuminant. After blooming (oxygenation), raw and salted meats were measured for 30 min at 4 °C. The colorimeter provided L^* (lightness), a^* (redness), and b^* (yellowness) values, which were obtained based on the three-dimensional color measurement criteria set forth by the International Commission on Illumination (Commision Internationale de l'Eclairage).

2.7. Shrinkage Rate

The shrinkage rate, serving as an indicator of surface change, was determined by measuring the diameter and thickness of salted and dried meats separately. To account for any possible deformation in the shape during drying, sample dimensions were measured with a digital vernier caliper (±0.1 mm) at multiple points along the major axes. The calculation of the shrinkage rate was calculated using Equation (1) [35]:

$$Shrinkage\ Rate\ (\%) = \frac{(SH - DH) + (SW - DW) + (SD - DD)}{SH + SW + SD} \quad (1)$$

where SH and DH denote the sample height in the salted and dried states, respectively; SW and DW refer to the sample width in the salted and dried states, respectively; and SD and DD denote the sample depth in the salted and dried states, respectively.

2.8. Microstructural Imaging

Microstructures of the dried samples were examined at the Central Research Laboratory (NABILTEM) of Tekirdağ Namık Kemal University. For this analysis, the samples were cut parallel to the muscle fibers. Subsequently, the prepared samples were placed in a scanning electron microscope (Quanta FEG 250, FEI, Hillsboro, OR, USA) and imaged with an LFD detector under low vacuum conditions at 90 Pa pressure and 5.0 kV voltage.

2.9. Rehydration Rate

After weighing, the dried meat samples were placed in a glass beaker containing 50 mL of water until they reached constant weight. The samples were then rehydrated in a 90 °C water bath. Excess water on the surface was dried, and the weights of the samples after rehydration were measured. The rehydration rate (%) was determined using Equation (2) [36]:

$$Rehydration\ Rate = \frac{M}{M_0} \tag{2}$$

where M is the sample weight after rehydration and M_0 is the sample weight before rehydration.

2.10. Modeling of Drying Data

Moisture rate (MR) was calculated from sample weights measured at regular intervals during drying (Equation (3)) [37]:

$$MR = \frac{M_t - M_e}{M_0 - M_e} \tag{3}$$

where M_0 is the initial moisture content (kg water/kg dry matter), M_t is the moisture content (kg water/kg dry matter), and M_e is the equilibrium moisture content. The value of M_e is zero because it is relatively lower than M_0 or M_t [38]. Effective moisture diffusion coefficients were calculated using Fick's second diffusion model shown in Equation (4).

$$MR = \frac{8}{\pi^2} exp\left(-\frac{\pi^2 D_{eff} t}{4L^2}\right) \tag{4}$$

where D_{eff} is the effective moisture diffusion coefficient (m^2/s), t is the drying time (s), and L is half of the sample height (m). The temperature dependence of the effective diffusion coefficient was determined by the Arrhenius equation for HAD and ID methods (Equation (5)).

$$D_{eff} = D_0\ exp\left(\frac{E_a}{RT}\right) \tag{5}$$

where D_0 is the pre-exponential factor of the Arrhenius equation (m^2/s), E_a is the activation energy (j/mol), R is the ideal gas constant (j/molK), and T is the temperature in Kelvin. In MD processes, which are based on power and not on temperature, the modified form of the Arrhenius equation by Dadali and Özbek (Equation (6)) [39] was used.

$$D_{eff} = D_0\ exp\left(-\frac{E_{a^*} m}{P}\right) \tag{6}$$

where E_a is activation energy (W/g), m is raw sample weight (g), and P is microwave power (W). The drying data underwent modeling using 9 different models shown in Table 1. The R^2 coefficient was used to select the best model to represent the drying curves. Besides R^2, various statistical parameters such as reduced chi-square (χ^2) and root mean square error (RMSE) were used to evaluate the best fit. The regression parameters (k, k_0, k_1, a, b, c, g, h, n)

and coefficients (R^2) were calculated by nonlinear regression (SPSS Statistics 27, IBM Corp., Armonk, NY, USA). The reduced chi-square (χ^2) and RMSE values were calculated using Equations (7) and (8) [40].

$$\chi^2 = \frac{\sum_{i=1}^{N}\left(MR_{exp,i} - MR_{pre,i}\right)^2}{N - z} \quad (7)$$

$$RMSE = \left[\frac{1}{N}\sum_{i=1}^{N}\left(MR_{pre,i} - MR_{exp,i}\right)^2\right]^{1/2} \quad (8)$$

where $MR_{exp,i}$ and $MR_{pre,i}$ are the experimental and predicted moisture contents, N is the number of trials, and Z is the constant number of the drying model.

Table 1. Mathematical models used to analyze the drying data.

Model Names	Model	Ref.
Lewis (Newton)	MR = exp(–kt)	[41]
Page	MR = exp (–ktn)	[42]
Weibull	MR = a exp (–ktn)	[43]
Henderson and Pabis	MR = a exp (–(kt))	[44]
Modified Henderson and Pabis	MR = a exp (–kt) + b exp (–gt) + c exp (–ht)	[45]
Logarithmic	MR = a exp (–(kt)) + c	[46]
Two-term	MR = a exp ($–k_0$t) + b exp (($–k_1$t)	[47]
Wang and Singh	MR = 1 + at + bt2	[48]
Verma	MR = a exp (–kt) + (1–a) exp (–gt)	[49]

2.11. Statistical Analyses

Experiments were conducted in two independent replicates for each drying method. The data were examined for normal distribution using various methods, including Kurtosis-Skewness values, Q-Q graphs, histograms, and the Kolmogorov–Smirnov test. The results indicated that the data exhibited a normal distribution. Next, the homogeneity of variances was assessed using Levene's test. Following confirmation of homogeneity, the data were analyzed using analysis of variance (ANOVA). Significant differences between the means were determined using the Duncan multiple comparison test.

3. Results and Discussion

3.1. Proximate Composition and pH of Raw Material

The mean proximate composition of raw goose breast meat was as follows: dry matter 26.88 ± 0.54%, fat 1.95 ± 0.12%, protein 21.84 ± 0.51%, total mineral content 1.06 ± 0.03%, and pH value 5.82 ± 0.02%. Similarly, Öz and Çelik [50] reported proximate composition values for raw goose meat that were comparable to our results.

3.2. Color and TBARS

Color and TBARS values of raw, salted, and dried samples are presented in Table 2. The L^* value measured in raw goose meat was the highest among all groups, and salting was observed to cause a significant decrease in the L^* value of the product. A statistically significant difference ($p < 0.05$) was found between the L^* value of raw meat and all other groups. However, no statistically significant difference was observed between salted meat and the drying groups. Regarding the drying process, the highest average L^* value was measured in the samples dried by microwave treatment at 460 W, and this value was statistically different ($p < 0.05$) from those measured in the dried samples of ID65, HAD55, and HAD65. As observed in the L^* value, the highest a^* value was determined in raw meat, and a statistically significant difference ($p < 0.05$) was found between this group and all

other groups. Salting caused a significant decrease in the a^* value, reducing the average to 10.73. However, with the drying process, a further decrease in a^* value was observed, and a statistically significant difference ($p < 0.05$) was found between the salted meat group and all drying groups. By contrast, the differences among the average values of the drying groups were not significant. The lowest b^* value was observed in raw meat, while salting resulted in a significant increase in the b^* value of the meat ($p < 0.05$). No significant difference ($p > 0.05$) was found in average b^* values between samples dried by infrared and hot air methods, whereas microwave-dried samples showed higher b^* values than other methods ($p < 0.05$), which is largely consistent with Özbay and Sarıçoban's [51] results on microwave-dried meat. In a hot air-drying study, it was observed that increasing the drying temperature led to higher L^* values and lower a^* values in red meat samples [52].

Table 2. Color and TBARS values of raw, salted, and dried goose meat (mean ± SD; $n = 36$).

Drying Method	Temperature/Power	L^*	a^*	b^*	TBARS (mgMDA/kg)
Raw meat		39.08 ± 3.32 ^{c}	18.04 ± 1.23 ^{c}	5.76 ± 0.44 ^{a}	0.43 ± 0.01 ^{a}
Salted meat		29.41 ± 0.93 ^{ab}	10.73 ± 0.89 ^{b}	9.36 ± 0.64 ^{b}	0.49 ± 0.02 ^{b}
ID	55 °C	27.64 ± 0.12 ^{ab}	3.46 ± 0.40 ^{a}	8.75 ± 0.71 ^{b}	0.79 ± 0.02 ^{g}
	65 °C	27.12 ± 0.19 ^{a}	3.56 ± 0.20 ^{a}	8.90 ± 0.67 ^{b}	0.72 ± 0.07 ^{ef}
	75 °C	27.83 ± 0.40 ^{ab}	4.40 ± 0.31 ^{a}	8.91 ± 0.83 ^{b}	0.64 ± 0.04 ^{c}
HAD	55 °C	27.01 ± 0.90 ^{a}	3.48 ± 0.37 ^{a}	8.75 ± 0.66 ^{b}	0.91 ± 0.03 ^{i}
	65 °C	26.87 ± 0.37 ^{a}	3.78 ± 0.29 ^{a}	8.75 ± 1.04 ^{b}	0.84 ± 0.02 ^{h}
	75 °C	27.83 ± 0.32 ^{ab}	4.47 ± 0.22 ^{a}	8.91 ± 0.6 ^{b}	0.75 ± 0.02 ^{f}
MD	120 W	27.33 ± 0.23 ^{ab}	3.67 ± 0.21 ^{a}	12.36 ± 0.49 ^{d}	0.83 ± 0.03 ^{gh}
	350 W	28.88 ± 0.79 ^{ab}	3.88 ± 0.11 ^{a}	11.68 ± 0.52 ^{cd}	0.69 ± 0.02 ^{de}
	460 W	29.74 ± 0.78 ^{b}	4.54 ± 0.21 ^{a}	11.01 ± 0.62 ^{c}	0.67 ± 0.09 ^{cd}

a–i: Values marked with different letters in the same column indicate statistically significant differences ($p < 0.05$).

Lipid oxidation is an important factor in dried products, and processing conditions influence the oxidation reaction [53]. The TBARS value for meat products has to be below 2 mg MDA/kg [54]. In the present results, the lowest TBARS value was observed in raw meat, while salting was found to increase this value. This result can be attributed to the pro-oxidant effect of salt on meat lipids [26]. On the other hand, there was an increase in TBARS values measured after salting based on this result. All drying methods applied in the study increased the TBARS values of the product during the drying process. A statistically significant difference ($p < 0.05$) was found between the average TBARS values measured as a result of drying processes. Accordingly, the highest average TBARS values were determined at the lowest temperature (55 °C)/power (120 W) values, while the lowest average TBARS values were measured at the highest temperature (75 °C)/power (460 W) values. This change in TBARS is consistent with previous studies showing that faster IR and MW heating shortens exposure and can reduce secondary lipid oxidation compared to prolonged convective drying [31,55–57].

The shorter drying time resulting from increased temperature or power may reduce air exposure, limiting oxidative reactions—a finding consistent with Demiray et al.'s [31] findings showing that increasing drying temperature from 50 °C to 70 °C decreased TBARS values from 1.43 ± 0.05 to 1.09 ± 0.03 mg MDA/kg.

3.3. Shrinkage and Rehydration Parameters

The effect of drying on the shrinkage and rehydration rates is presented in Table 3. Overall, shrinkage results from myofibrillar shortening and connective tissue contraction

caused by a temperature increase, and these microstructural changes reduce porosity and water pathways, thereby reducing rehydration and altering tissue [58]. In the present results, the highest shrinkage rates were observed at the highest temperature/power settings (75 °C/460 W). This outcome could be attributed to faster drying, which aligns with Aksoy et al. [59] study on minced meat. According to the aforementioned study, increasing temperature (25 °C, 35 °C, 45 °C) increased shrinkage rates in vacuum and ultrasound-vacuum drying. However, in contrast to our results, Özbay and Sarıçoban [51] found that varying energy levels in MD did not significantly impact the shrinkage rate of meat samples. The highest mean rehydration rate was observed at 75 °C in both infrared and dry air ($p < 0.05$), followed by the samples dried at 65 °C. MD showed the lowest rehydration rates. Of note, rehydration rates can vary with the drying method. In line with our findings, a previous study on minced meat using vacuum drying, ultrasound-assisted vacuum drying, and freeze-drying reported rehydration rates above '1' in all groups, showing variations between drying methods [59]. Rehydration occurs when water moves inward from the surface of the dried meat and enters the spaces within the structure; rehydration of dried meats is affected by different factors such as the microstructure of the sample and the drying process [7].

Table 3. The effect of drying on shrinkage and rehydration parameters (mean ± SD; $n = 36$).

Drying Method	Temperature/Power	Shrinkage Rate	Rehydration Rate
ID	55 °C	17.01 ± 0.62 ^{a}	1.44 ± 0.03 ^{c}
	65 °C	21.18 ± 0.71 ^{c}	1.52 ± 0.02 ^{d}
	75 °C	25.95 ± 1.30 ^{e}	1.58 ± 0.02 ^{e}
HAD	55 °C	18.40 ± 0.86 ^{b}	1.38 ± 0.02 ^{b}
	65 °C	23.11 ± 0.43 ^{d}	1.51 ± 0.01 ^{d}
	75 °C	29.13 ± 1.21 ^{f}	1.62 ± 0.02 ^{e}
MD	120 W	24.93 ± 1.01 ^{e}	1.11 ± 0.04 ^{a}
	350 W	29.49 ± 0.71 ^{f}	1.36 ± 0.03 ^{b}
	460 W	31.00 ± 0.66 ^{g}	1.36 ± 0.05 ^{b}

a–g: Values marked with different letters in the same column indicate statistically significant differences ($p < 0.05$).

3.4. Microstructure

Figure 1 shows microstructure images of goose meat dried by different methods and temperatures. The images are consistent with previous findings on food materials [2,60]. The images were captured in a direction parallel to that of the muscle fibrils. Figure 1 also shows salt crystals added by the salting process. The gaps between the fiber bundles are the result of salting, dehydration of water and drying processes [61]. As can be seen in Figure 1, different drying methods and the applied temperature and power parameters yielded different results. Connective tissue deformations occurred during drying processes [62].

More specifically, MD-dried samples were more deformed as compared to other drying methods (Figure 1g–i). Although the drying time in MD is shorter than that of other techniques, the electromagnetic energy of MD penetrates directly into the inner parts of the samples and is absorbed there, which results in rapid and non-uniform temperature increases. This may be the cause of the observed deformation, as such uneven heating can also induce protein denaturation and thereby exacerbate structural damage. MD caused more damage to fiber bundles and connective tissues, particularly at 120 W as compared to 350 and 460 W, possibly due to longer application times.

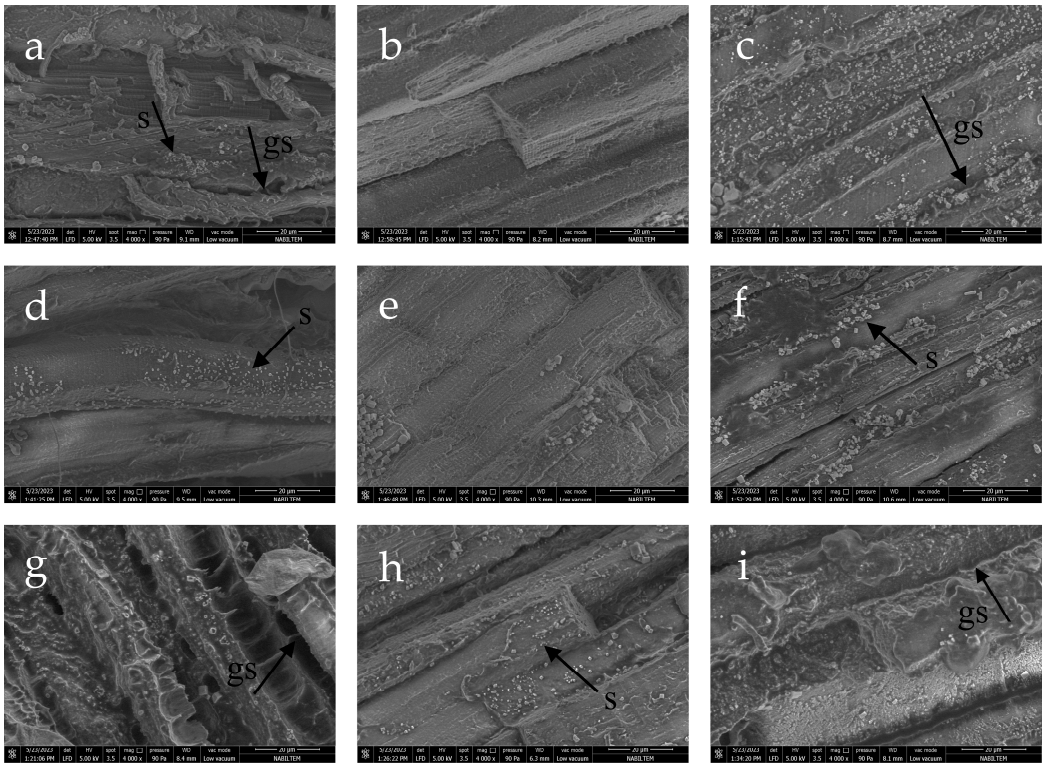

Figure 1. Microstructures of goose breast meats dried using different methods and temperatures ((**a**–**c**): 55, 65, 75 °C ID; (**d**–**f**): 55, 65, 75 °C HAD; (**g**–**i**): 120, 350, 460 W MD; s, salt; gs, gap size) ((**a**), (**b**) and (**c**) represent 55, 65, and 75 °C in ID, respectively; (**d**), (**e**), and (**f**) represent 55, 65, and 75 °C in HAD, respectively; (**g**), (**h**), and (**i**) represent 120, 350, and 460 W in MD, respectively).

Structural damage to the product during drying can cause the closure of microchannels and adversely affect rehydration capacity. In the present results, an inverse relationship was observed between the microstructural damage of dried products (Figure 1) and their rehydration capacity. Therefore, samples in which MD caused more severe microstructural damage exhibited lower rehydration properties. This is because a high rehydration capacity in a dried product requires minimal structural damage. Similarly, Prothon et al. [63] reported structural alterations and degradations in the cell wall after microwave-assisted drying, which consequently led to a reduction in rehydration capacity. Furthermore, Li et al. [64] reported that microwave heating of yak meat resulted in higher cooking loss, protein denaturation, and microstructural damage, leading to fiber fracture and contraction. In line with this evidence, the statistically significant increase in L^* values observed in our study may also be attributed to protein denaturation and fiber contraction caused by microwave treatment.

3.5. Drying Kinetics of Goose Meats

The drying curves of goose breast meat dried by different methods at different temperatures as a function of time are shown in Figure 2. The drying rate increased exponentially against time As documented in several previous studies [10,40], the drying rate increased exponentially against time. Drying was accelerated with increasing temperature in infrared and HAD and with increasing power in MD, which is largely consistent with the literature [32,65,66]. In addition, as can be seen in Figure 2, the ID process was faster at the same temperatures, and at 75 °C, the graphs coincided.

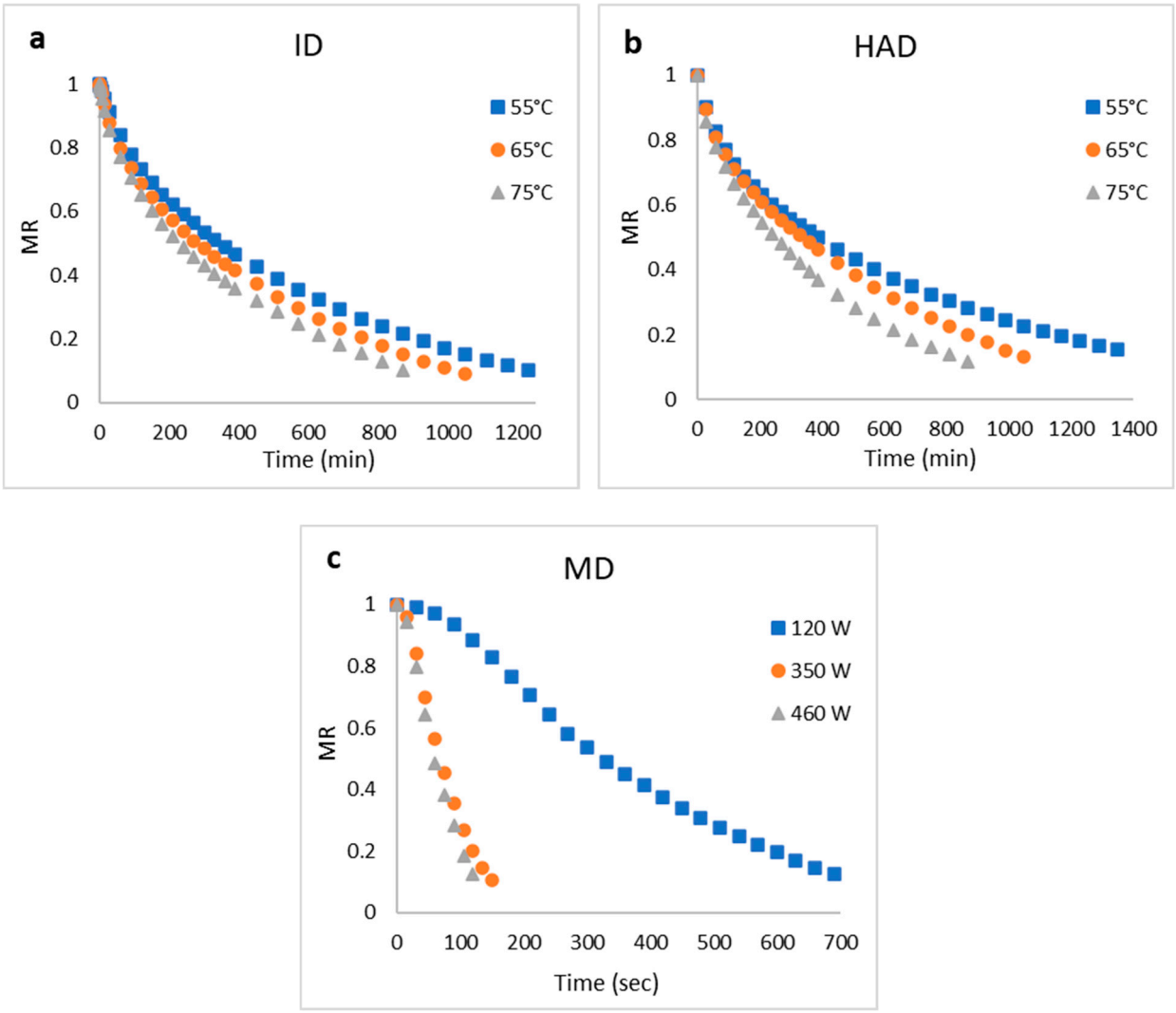

Figure 2. Drying curves of goose breast meat dried using different methods and temperatures. (**a**) ID, (**b**) HAD, (**c**) MD.

The estimated model parameters, coefficients of determination (R^2), chi-square (χ^2) and RMSE values obtained by applying the drying data to different kinetic models are reported in Table 4. High R^2 and low χ^2 and RMSE values determine how successful the model fit is. As can be seen from Table 4, the Weibull and Page models provided the best fit for the MD data, the two-term model for the HAD data, and the two-term together with the Verma model for the infrared data.

Mathematical models play a pivotal role in the analysis of the drying kinetics, which is the core of controlling the drying process and, thus, is of significant theoretical and practical importance in ensuring drying quality, reducing energy consumption, and optimizing the drying process. Dry-basis drying kinetics and their models are increasingly used to ensure effective process control. A close agreement between experimental kinetics and fitted models enables food engineers/technologists to monitor the process reliably, while the resulting drying data provide benchmarks for the development and optimization of alternative processes [29]. In this study, all models also exhibited high R^2 values and acceptable error levels, indicating that they represented the drying data quite well. In this context, the data in Table 4 provide comprehensive information for the drying sector.

Table 4. Estimated parameters obtained from kinetic models.

Model	Parameters	ID			HAD			MD		
		55 °C	65 °C	75 °C	55 °C	65 °C	75 °C	120 W	350 W	460 W
Lewis	k	0.116	0.141	0.167	0.099	0.122	0.160	8.058	39.904	45.251
	R^2	0.990	0.987	0.984	0.944	0.971	0.976	0.945	0.945	0.941
	$\chi^2 \times 10^3$	0.949	1.253	1.484	3.064	1.678	1.417	4.633	5.917	6.201
	RMSE	0.03034	0.034799	0.037808	0.054419	0.040139	0.036776	0.06734	0.073344	0.07424
Page	k	0.163	0.201	0.241	0.183	0.182	0.226	24.789	333.063	464.773
	n	0.839	0.817	0.790	0.727	0.799	0.807	1.504	1.565	1.592
	R^2	0.999	0.998	0.999	0.999	0.995	0.997	0.998	0.999	0.999
	$\chi^2 \times 10^3$	0.124	0.203	0.152	0.0783	0.266	0.168	0.166	0.0743	0.0878
	RMSE	0.01096	0.013998	0.012091	0.008698	0.015966	0.012668	0.01276	0.008219	0.008837
Weibull	a	1.001	0.997	1.001	0.990	0.976	0.978	1.024	1.012	1.007
	k	0.164	0.198	0.242	0.176	0.164	0.208	22.209	300.343	432.357
	n	0.838	0.821	0.789	0.738	0.835	0.838	1.440	1.533	1.571
	R^2	0.999	0.998	0.999	0.999	0.996	0.998	0.999	1.000	0.999
	$\chi^2 \times 10^3$	0.124	0.205	0.136	0.075	0.232	0.137	0.11	0.0538	0.0777
	RMSE	0.01098	0.014092	0.011427	0.008516	0.014922	0.011424	0.01040	0.006992	0.008312
Henderson and Pabis	k	0.111	0.133	0.157	0.083	0.107	0.143	9.444	44.809	50.480
	a	0.966	0.960	0.957	0.887	0.918	0.922	1.138	1.108	1.097
	R^2	0.993	0.991	0.990	0.983	0.990	0.992	0.977	0.965	0.960
	$\chi^2 \times 10^3$	0.623	0.797	0.948	0.94	0.548	0.471	1.946	3.735	4.242
	RMSE	0.02458	0.027765	0.030208	0.030148	0.022933	0.021198	0.04364	0.058274	0.061406
Modified Henderson and Pabis	a	−0.531	0.615	−0.547	0.781	0.626	0.610	3.432	−14.588	7.613
	b	5.058	−0.908	4.792	−1.643	−1.327	−1.290	2.211	7.091	5.328
	c	−4.532	0.262	−4.253	0.779	0.628	0.613	−5.564	7.554	−12.896
	h	−0.005	−0.005	−0.007	−0.004	−0.004	−0.005	0.912	8.964	2.723
	g	0.300	0.142	0.496	0.095	0.108	0.146	2.846	8.949	8.108
	k	0.301	−0.005	0.497	−0.004	−0.003	−0.005	2.844	2.948	8.266
	R^2	0.999	0.993	0.999	0.989	0.991	0.993	0.994	0.991	0.992
	$\chi^2 \times 10^3$	0.058	0.67	0.0681	0.608	0.533	0.426	0.537	0.942	0.861
	RMSE	0.00751	0.02545	0.008095	0.024234	0.022631	0.020163	0.02292	0.02926	0.027673
Logarithmic	a	0.904	0.900	0.875	0.796	0.874	0.879	1.684	1.840	2.512
	k	0.133	0.158	0.200	0.121	0.124	0.166	4.501	18.339	14.144
	c	0.073	0.070	0.096	0.130	0.057	0.059	−0.605	−0.784	−1.649
	R^2	0.995	0.994	0.994	0.991	0.992	0.994	0.993	0.991	0.992
	$\chi^2 \times 10^3$	0.415	0.595	0.586	0.492	0.489	0.381	0.568	0.989	0.878
	RMSE	0.02006	0.02398	0.023751	0.02181	0.021669	0.019071	0.02357	0.029986	0.027933
Two-term	k_1	1.062	1.584	1.563	0.863	1.615	2.252	2.818	11.085	8.499
	k_2	0.097	0.116	0.132	0.072	0.099	0.133	2.427	9.845	7.014
	a	0.131	0.141	0.165	0.204	0.137	0.131	12.583	18.753	19.006
	b	0.873	0.863	0.837	0.796	0.865	0.869	−11.504	−17.697	−17.962
	R^2	1.000	0.999	1.000	1.000	0.999	1.000	0.993	0.991	0.992
	$\chi^2 \times 10^3$	0.036	0.0563	0.043	0.00209	0.0614	0.00885	0.549	0.982	0.875
	RMSE	0.0059	0.007376	0.006433	0.001423	0.007676	0.002906	0.02318	0.029878	0.027894
Wang and Singh	a	−0.099	−1.118	−0.142	−0.090	−0.108	−0.138	−5.536	−28.041	−30.469
	b	0.003	0.004	0.006	0.002	0.004	0.006	5.222	137.166	99.316
	R^2	0.997	0.971	0.969	0.931	0.952	0.956	0.985	0.987	0.988
	$\chi^2 \times 10^3$	2.174	2.705	2.793	3.788	2.743	2.623	1.231	1.432	1.218
	RMSE	0.04592	0.051136	0.051864	0.060516	0.051318	0.050036	0.03471	0.036076	0.032907
Verma	k	0.097	0.116	0.132	0.099	0.099	0.133	0.864	5.401	2.795
	a	0.872	0.862	0.836	−0.429	0.865	0.869	−10.462	−16.853	−17.751
	g	1.002	1.490	1.511	0.099	1.594	2.251	1.288	6.669	4.267
	R^2	1.000	0.999	1.000	0.944	0.999	1.000	0.985	0.986	0.988
	$\chi^2 \times 10^3$	0.038	0.0588	0.0433	3.066	0. 0618	0. 00885	1.261	1.493	1.237
	RMSE	0.00604	0.007539	0.006461	0.054444	0.007704	0.002906	0.03514	0.036845	0.033157

For both infrared and HAD, the drying rate constant (k) consistently increased with rising temperature, whereas for MD it increased with increasing microwave power, indicating that higher temperatures or powers accelerated moisture removal. However, the k values obtained in MD were considerably higher than those of HAD and infrared drying, which can be attributed to the direct penetration of microwave energy into the inner parts of the material and the rapid heating of water molecules, resulting in faster moisture diffusion and evaporation [40,59,60].

Effective moisture diffusion (D_{eff}), an important concept for the determination of physical and thermal properties, is defined as the transport of moisture at a decreasing rate period during drying [67]. D_{eff} values varied with increasing temperature in infrared and HAD, and with applied power in MD (Table 4). MD had higher D_{eff} values, indicating more effective heat distribution and convection [65]. Activation energy is defined as the energy required to remove moisture from a solid [68]. Activation energies for drying were 17,169.91 J/mol in ID, 24,526.51 J/mol in HAD, and 26.98 W/g in MD (Table 5). ID was less sensitive to temperature changes as compared to HAD, as indicated by lower activation energy in ID.

Table 5. Effective moisture diffusion and Arrhenius equation parameters of drying techniques.

Drying Method	D_{eff} (m^2/s)	Arrhenius Parameters		
		D_0	Ea (J/mol)	R^2
ID	2.44×10^{-10} 2.97×10^{-10} 3.51×10^{-10}	1.325×10^{-7}	17,169.91	0.999
HAD	2.05×10^{-10} 2.52×10^{-10} 3.38×10^{-10}	1.601×10^{-6}	24,526.51	0.988
MD	1.71×10^{-8} 8.72×10^{-8} 9.74×10^{-8}	1.802×10^{-7}	26.98 (W/g)	0.993

4. Conclusions

The results of the present study revealed that drying methods and operating parameters significantly affect both product quality attributes and drying time. Increasing temperature (HAD/IR) or microwave power (MD) accelerated moisture removal, and MD achieved the shortest drying times. SEM micrographs revealed inter-fibrillar gaps formed due to water removal and method-dependent degrees of fiber damage; these microstructural changes were probably associated with rehydration capacity and color attributes. Therefore, the drying method together with its set-points (temperature/power) jointly determined the trade-off between process time and quality attributes, allowing conditions to be tuned to a targeted quality profile.

To conclude, the present study provided relevant evidence to guide the selection of the appropriate drying method according to target product attributes and processing conditions, rather than promoting a single best technique. The findings also offer practical guidance for the food industry and for food engineers and technologists in tailoring method choice to specific constraints (e.g., prioritizing rehydration quality and structural integrity versus throughput and process economy). For instance, our findings demonstrate that MD achieved shorter drying times (i.e., higher drying-rate constants, k) than the other techniques, whereas HAD and IR were superior in rehydration capacity and preservation of microstructure. Accordingly, in contexts where rehydration performance

and structural integrity are critical, HAD or IR are preferable; conversely, when throughput and process economy are prioritized, MD can be advantageous despite its microstructural drawbacks. Overall, this study provides a comprehensive comparative assessment and supports application-specific selection of the drying method.

Author Contributions: Conceptualization, E.K. and M.A.Ç.; methodology, E.K. and M.A.Ç.; validation, E.K. and M.A.Ç.; formal analysis, E.K. and M.B.; investigation, E.K., M.A.Ç., B.Y. and M.B.; resources, E.K. and B.Y.; data curation, E.K. and M.B.; writing—original draft preparation, E.K., B.Y. and M.B.; writing—review and editing, E.K., B.Y. and M.B.; visualization, E.K. and M.B.; supervision, E.K.; project administration, E.K.; funding acquisition, E.K. All authors have read and agreed to the published version of the manuscript.

Funding: This research was supported by Yalova University's Scientific Research Projects Coordination Unit by project number 2021/AP/0011.

Data Availability Statement: The original contributions presented in this study are included in the article. Further inquiries can be directed to the corresponding author.

Conflicts of Interest: Author Mehmet Başlar was employed by iPeak Academy Ltd. The remaining authors declare that the research was conducted in the absence of any commercial or financial relationships that could be construed as a potential conflict of interest.

References

1. Aykın Dinçer, E.; Erbaş, M. Kurutulmuş et ürünlerinin kalite özellikleri. *Gıda* **2019**, *44*, 472–482. [CrossRef]
2. Başlar, M.; Yalınkılıç, B.; Erol, K.F.; İrkilmez, M.Ü. Evaluation of the Use of Vacuum-Dehydrated Minced Meat in Beef Patty Production. *AgriEngineering* **2024**, *6*, 1712–1724. [CrossRef]
3. Álvarez, S.; Álvarez, C.; Hamill, R.; Mullen, A.M.; O'Neill, E. Drying Dynamics of Meat Highlighting Areas of Relevance to Dry-Aging of Beef. *Compr. Rev. Food Sci. Food Saf.* **2021**, *20*, 5370–5392. [CrossRef]
4. Göztok, S.P.; İçier, F. Karbon Fiber Destekli Kabin Kurutucuda Farklı Sıcaklıklarda Elma Dilimlerinin Kurutulmasının İncelenmesi: Kurutma Karakteristikleri ve Performans Değerlendirmesi. *Akad. Gıda* **2017**, *15*, 355–367. [CrossRef]
5. Li, Y.; Zhang, J.; Wang, J.; Ren, J.; Cao, C.; Liu, Q.; Huang, X. Evaluation of Drying Characteristics and Quality Attributes for Microwave Vacuum Drying of Pork Skin Crisps. *Foods* **2024**, *13*, 4020. [CrossRef]
6. Bassey, E.J.; Cheng, J.H.; Sun, D.W. Improving Drying Kinetics, Physicochemical Properties and Bioactive Compounds of Red Dragon Fruit (*Hylocereus* Species) by Novel Infrared Drying. *Food Chem.* **2022**, *375*, 131886. [CrossRef]
7. Ren, Y.; Sun, D.W. Monitoring of Moisture Contents and Rehydration Rates of Microwave Vacuum and Hot Air Dehydrated Beef Slices and Splits Using Hyperspectral Imaging. *Food Chem.* **2022**, *382*, 132346. [CrossRef]
8. Wang, Q.; Li, S.; Han, X.; Ni, Y.; Zhao, D.; Hao, J. Quality Evaluation and Drying Kinetics of Shiitake Mushrooms Dried by Hot Air, Infrared and Intermittent Microwave-Assisted Drying Methods. *LWT* **2019**, *107*, 236–242. [CrossRef]
9. Wang, Y.; Li, Y.; Pan, S.; Qin, M.; Yuan, Y.; Li, C.; Liu, Y. Effects of Infrared Radiation Parameters on Drying Characteristics and Quality of Rice: A Systematic Review. *Food Bioproc. Technol.* **2025**, *18*, 6813–6835. [CrossRef]
10. Aykın Dinçer, E.; Kılıç-Büyükkurt, Ö.; Erbaş, M. Influence of Drying Techniques and Temperatures on Drying Kinetics and Quality Characteristics of Beef Slices. *Heat Mass Transf.* **2020**, *56*, 315–320. [CrossRef]
11. An, N.N.; Li, D.; Wang, L.J.; Wang, Y. Factors Affecting Energy Efficiency of Microwave Drying of Foods: An Updated Understanding. *Crit. Rev. Food Sci. Nutr.* **2024**, *64*, 2618–2633. [CrossRef]
12. Demiray, E.; Seker, A.; Tulek, Y. Drying Kinetics of Onion (*Allium cepa* L.) Slices with Convective and Microwave Drying. *Heat Mass Transf.* **2017**, *53*, 1817–1827. [CrossRef]
13. Fekete, S.; Jónás, G.; Felföldi, J.; Kovacs, Z.; Friedrich, L. Investigation of Salt and Water Diffusion during Dry Salting, Wet Curing, and Ultrasonic Wet Curing. *Appl. Sci.* **2025**, *15*, 5939. [CrossRef]
14. Yalınkılıç, B.; Kaban, G.; Ertekin, Ö.; Kaya, M. Determination of Volatile Compounds of Sucuk with Different Orange Fiber and Fat Levels. *Kafkas Univ. Vet. Fak. Derg.* **2015**, *21*, 233–239. [CrossRef]
15. Yalınkılıç, B.; Kaban, G.; Kaya, M. Effect of Sodium Replacement on the Quality Characteristics of Pastırma (a Dry-Cured Meat Product). *Food Sci. Hum. Wellness* **2023**, *12*, 266–274. [CrossRef]
16. Ceviker, C.; Karakose, C.; Kahraman, G.; Aydin, N.; Öztürk, İ. Physicochemical and Microbiological Properties of Different Kayseri Pastirma Types. *Int. J. Gastron. Res.* **2025**, *4*, 1–6. [CrossRef]
17. FAO. *FAOSTAT: Crops and Livestock Products*; Food and Agriculture Organization of the United Nations: Rome, Italy, 2024. Available online: https://www.fao.org/faostat/en/#data/QCL (accessed on 20 September 2025).

18. Molnár, S. Evaluation of the Hungarian and Polish goose meat production. *Roczniki* **2017**, *2016*, 255–261. [CrossRef]
19. Yan, L.; Liu, J.; Chen, R.; Lei, M.; Guo, B.; Chen, Z.; Zhu, H. Reproductive Characteristics and Methods to Improve Reproductive Performance in Goose Production: A Systematic Review. *Poult. Sci.* **2025**, *104*, 105099. [CrossRef] [PubMed]
20. Çimen, H.; Kızılkaya, P.; Sayın, B.; Baltakesmez, D.A.; Kırmacı, F. Goose Meat: Salting/Drying Effect on Nutritional Value, Physicochemical Properties, and Sensory Properties. *Gıda Yem Bilim. Teknol. Derg.* **2025**, *33*, 40–50. [CrossRef]
21. Taste Atlas. Most Popular Goose Dishes in the World. Available online: https://www.tasteatlas.com/most-popular-goose-dishes-in-the-world (accessed on 1 August 2023).
22. Kaban, G.; Kızılkaya, P.; Börekçi, B.S.; Hazar, F.Y.; Kabil, E.; Kaya, M. Microbiological Properties and Volatile Compounds of Salted-Dried Goose. *Poult. Sci.* **2020**, *99*, 2293–2299. [CrossRef]
23. Nowicka, K.; Jaworska, D.; Przybylski, W.; Górska, E.; Tambor, K.; Poltorak, A. Determinants of the Sensory Quality of Półgęsek in Relation to Volatile Compounds and Chemical Composition. *Pol. J. Food Nutr. Sci.* **2017**, *67*, 283–292. [CrossRef]
24. Gülbaz, G.; Kamber, U. Experimentally Fermented Sausage from Goose Meat and Quality Attributes. *J. Muscle Foods* **2008**, *19*, 247–260. [CrossRef]
25. Güner, A.; Doğruer, Y.; Uçar, G.; Yörük, H.D. The Possibility of Using Goose Meat in the Production of Salami. *Turk. J. Vet. Anim. Sci.* **2002**, *26*, 1303–1308.
26. Feiner, G. *Meat Products Handbook: Practical Science and Technology*; CRC Press: New York, NY, USA, 2006.
27. Kabil, E.; Hazar Suncak, F.Y.; Kaban, G.; Kaya, M. Effect of Low-Salt Processing on Lipolytic Activity, Volatile Compound Profile, Color, Lipid Oxidation, and Microbiological Properties of Four Different Types of Pastırma. *Appl. Sci.* **2025**, *15*, 8343. [CrossRef]
28. Lesiow, T. Chemical Composition of Poultry Meat. In *Handbook of Food Science, Technology, and Engineering*; Hui, Y.H., Ed.; CRC Press: London, UK, 2006; pp. 32-1–32-21.
29. Çakır, M.A.; Kabil, E.; Yalınkılıç, B.; Başlar, M. Investigation of Drying Kinetics of Turkey Breast Meat Using Vacuum and Ultrasound-Assisted Vacuum Drying. *Int. J. Agric. Environ. Food Sci.* **2025**, *9*, 725–732. [CrossRef]
30. Rao, W.; Wang, Z.; Li, G.; Meng, T.; Suleman, R.; Zhang, D. Formation of Crust of Dried Meat and Its Relationship to Moisture Migration during Air Drying. *J. Food Process. Preserv.* **2020**, *44*, e14255. [CrossRef]
31. Demiray, E.; Özünlü, O.; Ergezer, H.; Gökçe, R. Influence of hot-air drying on drying kinetics and some quality parameters of sliced chicken breast meat. *J. Therm. Anal. Calorim.* **2025**, *150*, 13231–13241. [CrossRef]
32. Elmas, F.; Bodruk, A.; Köprüalan, Ö.; Arıkaya, Ş.; Koca, N.; Serdaroğlu, F.M.; Kaymak-Ertekin, F.; Koç, M. Drying Kinetics Behavior of Turkey Breast Meat in Different Drying Methods. *J. Food Process Eng.* **2020**, *43*, e13487. [CrossRef]
33. Gökalp, H.Y.; Kaya, M.; Zorba, Ö.; Tülek, Y. *Et Ürünlerinde Kalite Kontrolü ve Laboratuvar Uygulama Kılavuzu*; Atatürk Üniversitesi Ziraat Fakültesi Ofset Tesisi: Erzurum, Türkiye, 1999.
34. Lemon, D.W. An Improved TBA Test for Rancidity. In *New Series Circular No: 51*; Halifax Laboratory: Halifax, NS, Canada, 1975.
35. Yalınkılıç, B. Effects of Different Chloride Salts and Fat Levels on the Quality Characteristics of Beef Patties. *Int. J. Gastron. Res.* **2024**, *3*, 84–91. [CrossRef]
36. Doymaz, İ.; İsmail, O. Drying and Rehydration Behaviors of Green Bell Peppers. *Food Sci. Biotechnol.* **2010**, *19*, 1449–1455. [CrossRef]
37. Midilli, A.; Kucuk, H.; Yapar, Z. A New Model for Single-Layer Drying. *Dry. Technol.* **2002**, *20*, 1503–1513. [CrossRef]
38. Kingsly, A.R.P.; Singh, D.B. Drying Kinetics of Pomegranate Arils. *J. Food Eng.* **2007**, *79*, 741–744. [CrossRef]
39. Dadali, G.; Özbek, B. Microwave Heat Treatment of Leek: Drying Kinetic and Effective Moisture Diffusivity. *Int. J. Food Sci. Technol.* **2008**, *43*, 1443–1451. [CrossRef]
40. Başlar, M.; Kılıçlı, M.; Yalınkılıç, B. Dehydration Kinetics of Salmon and Trout Fillets Using Ultrasonic Vacuum Drying as a Novel Technique. *Ultrason. Sonochem.* **2015**, *27*, 495–502. [CrossRef]
41. Bruce, D.M. Exposed-Layer Barley Drying: Three Models Fitted to New Data up to 150 °C. *J. Agric. Eng. Res.* **1985**, *32*, 337–348. [CrossRef]
42. Madamba, P.S.; Driscoll, R.H.; Buckle, K.A. The Thin-Layer Drying Characteristics of Garlic Slices. *J. Food Eng.* **1996**, *29*, 75–97. [CrossRef]
43. Ojha, K.S.; Kerry, J.P.; Tiwari, B.K. Investigating the Influence of Ultrasound Pre-Treatment on Drying Kinetics and Moisture Migration Measurement in *Lactobacillus sakei* Cultured and Uncultured Beef Jerky. *LWT* **2017**, *81*, 42–49. [CrossRef]
44. Henderson, S.M.; Pabis, S. Grain Drying Theory II: Temperature Effects on Drying Coefficients. *J. Agric. Eng. Res.* **1961**, *6*, 169–174.
45. Karathanos, V.T. Determination of Water Content of Dried Fruits by Drying Kinetics. *J. Food Eng.* **1999**, *39*, 337–344. [CrossRef]
46. Toğrul, İ.T.; Pehlivan, D. Modelling of Drying Kinetics of Single Apricot. *J. Food Eng.* **2003**, *58*, 23–32. [CrossRef]
47. Henderson, S.M. Progress in Developing the Thin Layer Drying Equation. *Trans. ASAE* **1974**, *17*, 1167–1168. [CrossRef]
48. Wang, C.Y.; Singh, R.P. A Single Layer Drying Equation for Rough Rice. In *ASAE Paper No. 78-3001*; American Society of Agricultural Engineers: St. Joseph, MI, USA, 1978; p. 33.
49. Verma, L.R.; Bucklin, R.A.; Endan, J.B.; Wratten, F.T. Effects of Drying Air Parameters on Rice Drying Models. *Trans. ASAE* **1985**, *28*, 296–301. [CrossRef]

50. Oz, F.; Celik, T. Proximate composition, color and nutritional profile of raw and cooked goose meat with different methods. *J. Food Process. Preserv.* **2015**, *39*, 2442–2454. [CrossRef]
51. Özbay, S.; Sariçoban, C. Effects of Different Levels of Salt and Temperature on Some Physico-Chemical and Colour Properties of Microwave-Dried Beef Round (*M. semitendinosus*). *Br. Food J.* **2021**, *123*, 2066–2078. [CrossRef]
52. von Gersdorff, G.J.; Kirchner, S.M.; Hensel, O.; Sturm, B. Impact of Drying Temperature and Salt Pre-Treatments on Drying Behavior and Instrumental Color and Investigations on Spectral Product Monitoring during Drying of Beef Slices. *Meat Sci.* **2021**, *178*, 108525. [CrossRef] [PubMed]
53. Oz, E.; Kabil, E.; Kaya, M. The Effects of Curing Agents on the Proteolysis and Lipid Oxidation of Pastırma Produced by the Traditional Method. *J. Food Sci. Technol.* **2021**, *58*, 2806–2814. [CrossRef] [PubMed]
54. Greene, B.E.; Cumuze, T.H. Relationship between TBA Numbers and Inexperienced Panelists' Assessments of Oxidized Flavor in Cooked Beef. *J. Food Sci.* **1982**, *47*, 52–54. [CrossRef]
55. Kipcak, A.S.; Ismail, O. Microwave Drying of Fish, Chicken and Beef Samples. *J. Food Sci. Technol.* **2021**, *58*, 281–291. [CrossRef]
56. Mediani, A.; Hamezah, H.S.; Jam, F.A.; Mahadi, N.F.; Chan, S.X.Y.; Rohani, E.R.; Abas, F. A Comprehensive Review of Drying Meat Products and the Associated Effects and Changes. *Front. Nutr.* **2022**, *9*, 1057366. [CrossRef]
57. Ying, W.; Ya-Ting, J.; Jin-Xuan, C.; Yin-Ji, C.; Yang-Ying, S.; Xiao-Qun, Z.; Ning, G. Study on Lipolysis-Oxidation and Volatile Flavour Compounds of Dry-Cured Goose with Different Curing Salt Content during Production. *Food Chem.* **2016**, *190*, 33–40. [CrossRef]
58. Shi, S.; Feng, J.; An, G.; Kong, B.; Wang, H.; Pan, N.; Xia, X. Dynamics of Heat Transfer and Moisture in Beef Jerky during Hot Air Drying. *Meat Sci.* **2021**, *182*, 108638. [CrossRef]
59. Aksoy, A.; Karasu, S.; Akcicek, A.; Kayacan, S. Effects of Different Drying Methods on Drying Kinetics, Microstructure, Color, and the Rehydration Ratio of Minced Meat. *Foods* **2019**, *8*, 216. [CrossRef] [PubMed]
60. Başlar, M. From Fresh to Dried: Evaluating Drying Kinetics of Sultana and Besni Grapes. *Int. J. Gastron. Res.* **2023**, *2*, 37–41. [CrossRef]
61. Bampi, M.; Schmidt, F.C.; Laurindo, J.B. A Fast Drying Method for the Production of Salted-and-Dried Meat. *Food Sci. Technol.* **2019**, *39*, 526–534. [CrossRef]
62. Nathakaranakule, A.; Kraiwanichkul, W.; Soponronnarit, S. Comparative Study of Different Combined Superheated-Steam Drying Techniques for Chicken Meat. *J. Food Eng.* **2007**, *80*, 1023–1030. [CrossRef]
63. Prothon, F.; Ahrné, L.M.; Funebo, T.; Kidman, S.; Langton, M.; Sjöholm, I. Effects of Combined Osmotic and Microwave Dehydration of Apple on Texture, Microstructure and Rehydration Characteristics. *LWT* **2001**, *34*, 95–101. [CrossRef]
64. Li, S.; Tang, S.; Yan, L.; Li, R. Effects of microwave heating on physicochemical properties, microstructure and volatile profiles of yak meat. *J. Appl. Anim. Res.* **2019**, *47*, 262–272. [CrossRef]
65. Ahmat, T.; Barka, M.; Aregba, A.W.; Bruneau, D. Convective Drying Kinetics of Fresh Beef: An Experimental and Modeling Approach. *J. Food Process. Preserv.* **2015**, *39*, 2581–2595. [CrossRef]
66. İsmail, O.; Kocabay, O. Infrared and Microwave Drying of Rainbow Trout: Drying Kinetics and Modelling. *Turk. J. Fish. Aquat. Sci.* **2018**, *18*, 259–266. [CrossRef]
67. Minaei, S.; Motevali, A.; Ahmadi, E.; Azizi, H. Mathematical Models of Drying Pomegranate Arils in Vacuum and Microwave Dryers. *J. Agric. Sci. Technol.* **2012**, *14*, 311–325.
68. Mirzaee, E.; Rafiee, S.; Keyhani, A.; Emam-Djomeh, Z. Determining of Moisture Diffusivity and Activation Energy in Drying of Apricots. *Res. Agric. Eng.* **2009**, *55*, 114–120. [CrossRef]

Disclaimer/Publisher's Note: The statements, opinions and data contained in all publications are solely those of the individual author(s) and contributor(s) and not of MDPI and/or the editor(s). MDPI and/or the editor(s) disclaim responsibility for any injury to people or property resulting from any ideas, methods, instructions or products referred to in the content.